Electronic Supplementary Information

Label-free and sensitive detection of RNA demethylase FTO with primer generation rolling circle amplification

Xiaoxia Han,‡[a] Yueying Li,‡[b] Zi-yue Wang,‡[b] Ling-Zhi Liu,[c] Jian-Ge Qiu,[a] Bing-Jie Liu,*[a] Chun-yang Zhang *[b]

[a] BGI College & Henan Institute of Medical and Pharmaceutical Sciences, Academy of Medical Sciences, Zhengzhou University, Zhengzhou 450000, China.

[b] College of Chemistry, Chemical Engineering and Materials Science, Shandong Normal University, Jinan 250014, China.

[c] Department of Oncology, Thomas Jefferson University, Philadelphia, PA, USA

* Corresponding author. Tel.: +86 0531-86186033; Fax: +86 0531-82615258. E-mail: bingjieliu@zzu.edu.cn, cyzhang@sdnu.edu.cn.

‡ These authors contributed equally.

EXPERIMENTAL SECTION

Materials

All oligonucleotides (Table S1) were synthesized by Sangon Biotechnology Co. Ltd. (Shanghai, China). FTO was purchased from Active Motif (Carlsbad, CA, USA). MazF mRNA intereferase (MazF) was obtained from TAKARA Bio. (Dalian, China). Ammonium iron (II) sulfate haxahydrate ($(NH_4)_2Fe(SO_4)_2$), α-ketoglutaric acid, ammonium sulfate ($(NH_4)_2SO_4$), magnesium chloride ($MgCl_2$), 4-(2-hydroxyethyl)-piperazine-1-ethanesulfonic acid sodium salt (HEPES), bovine serum albumin (BSA), and nuclease-free water were purchased from Sigma-Aldrich (St. Louis, MO, USA). Diacerein, rhein and L-ascorbic acid were purchased from Aladdin (Beijing, China). T4 polynucleotide kinase, Nb. BsmI, dNTP and vent (exo-) DNA polymerase were purchased from New England Biolabs (Ipswich, MA, USA).

Table 1. Sequences of the oligonucleotides [α]

note	Sequence (5'-3')
RNA probe	*GCA AUC GUA UCU UCU CG*^{m}A CAU UUA AAA AA-NH_2
Circular template	TGA CCC ACC CAC CCA CCC ACA <u>GAA TGC</u> TGA CCC ACC CAC CCA CCC ACA <u>GAA TGC</u> TGT **CGA GAA GAT ACG ATT GC**

[α] In the RNA probe, the binding region of circular template is shown in italic. In the circular template, the binding region of primer is shown in boldface, and the nicking site is shown in the underline.

In vitro FTO assay

The demethylation activity assay was performed in 20 μL of reaction mixture containing 500 nM

RNA probes, varying concentrations of FTO protein, and 1× FTO reaction buffer (50 mM HEPES (pH 7.5), 100 μM α-ketoglutaric acid, 100 μM L-ascorbic acid and 150 μM $(NH_4)_2Fe(SO_4)_2$) at 30 ℃ for 90 min, and the reaction was terminated by inactivation at 95 ℃ for 5 min. After demethylation reaction, 10 μL of reaction products was incubated with 10 U of MazF in MazF reaction buffer (40 mM sodium phosphate (pH 7.5), 0.01% Tween-20, and 5 mM EDTA) at 37 °C for 90 min. Then the dephosphorylation reaction was performed at 37 ℃ for 5 h in 30 μL of reaction mixtures containing 1 μL of 10 U/μL T4 PNK, 3 μL of 10× T4 PNK reaction buffer (70 mM Tris-HCl, 10 mM $MgCl_2$, 5 mM DTT, pH 7.6), 6 μL of H_2O and 20 μL of digestion products. The reaction was terminated by inactivation at 65 ℃ for 20 min. The primer generation rolling circle amplification (PG-RCA) reaction was performed at 45 °C for 2 h in 50 μL of reaction solution containing 5 μL of 10× thermopol reaction buffer (20 mM Tris−HCl buffer, 10 mM $(NH_4)_2SO_4$, 10 mM KCl, 2 mM $MgSO_4$, 0.1% Triton X-100, pH 8.8), 600 μM dNTP, 60 nM circular template, 0.8 U of Vent (exo-) DNA polymerase, 15 U of Nb. BsmI, and 30 μL of dephosphorylation reaction products. The 50 μL of amplification reaction products was diluted to a final volume of 80 μL with pure water and stained with 1× SYBR Gold. The fluorescence spectra were measured using a trace quartz cuvette on a Hitachi F-7000 fluorescence spectrophotometer (Tokyo, Japan) with an excitation wavelength of 488 nm. The emission spectra were recorded over the wavelength range of 500 – 700 nm with a slit width of 5 nm for both excitation and emission. The fluorescence intensity at 556 nm was used for data analysis.

Gel Electrophoresis analysis

The products of cleavage reactions were stained with SYBR Gold and analyzed by 12% native

polyacrylamide gel electrophoresis (PAGE) in 1× TBE buffer (9 mM Tris-HCl, pH 8.3, 9 mM boric acid, 0.2 mM EDTA) at a 110 V constant voltage for 40 min. After electrophoresis, a photograph was taken in a Bio-Rad ChemiDoc MP Imaging System. The products of PG-RCA reaction were analyzed by 16% PAGE in 1× TBE buffer at a 150 V constant voltage for 60 min. After electrophoresis, a photograph was taken in a Bio-Rad ChemiDoc MP Imaging System by using an illumination source of Epi-blue (460 – 490 nm excitation) and a 516 – 544 nm filter for SYBR Gold fluorophore.

Inhibition assay

Different concentrations of different inhibitors were incubated with a solution containing 500 nM RNA probe, 0.1 nM FTO and 1× FTO reaction buffer (50 mM HEPES (pH 7.5), 100 μM α-ketoglutaric acid, 100 μM L-ascorbic acid and 150 μM $(NH_4)_2Fe(SO_4)_2$) at 30 ℃ for 1.5 h, and the reaction was terminated by inactivation at 95 ℃ for 5 min. The following experiment was carried out according to the procedures of FTO assay described above. The relative activity (*RA*) of FTO was calculated based on equation 1.

$$RA = \frac{C_i}{C_t} \times 100\ \% = 10^{(Y_i - Y_t)/1011.08} \times 100\ \% \qquad (1)$$

where Y_t represents the fluorescence intensity in the presence of 0.1 nM FTO, and Y_i represents the fluorescence intensity in the presence of 0.1 nM FTO + inhibitors. C_i and C_t were obtained according to the linear correlation equation (Fig. 2B), respectively. The IC_{50} value of inhibitor was obtained from the curve-fitting equation.

$$Y_t = 6714.61 + 1011.08 \log_{10} C_t \qquad (2)$$

$$Y_i = 6714.61 + 1011.08 \log_{10} C_i \qquad (3)$$

Cell culture and preparation of cytoplasm extracts

Human breast cancer cell line (MDA-MB-231 cells and MCF-7 cells), human cervical carcinoma cell line (HeLa cells), and human breast normal cells (MCF-10A cells) were purchased from Cell Bank of Chinese Academy of Sciences (Shanghai, China). MDA-MB-231 cells were grown on glass-bottom culture dishes in Leibovitz's L-15 Medium (Gibco, U.S.A.) supplemented with 10% fetal bovine serum and 1% penicillin-streptomycin. MCF-7 cells and HeLa cells were grown in Dulbecco's modified Eagle's medium supplemented with 10% fetal bovine serum and 1% penicillin/streptomycin. MCF-10A cells were cultivated in complete growth medium (Procell Life Science & Technology Co., Ltd.). The cells were incubated at 37 ℃ in a humidified chamber with 5% CO_2. The cytoplasm lysates were obtained by using the nuclear extract kit (Active Motif, Carlsbad, CA, USA) according to the manufacturer's protocol. The resultant supernatant was subjected to FTO assays.

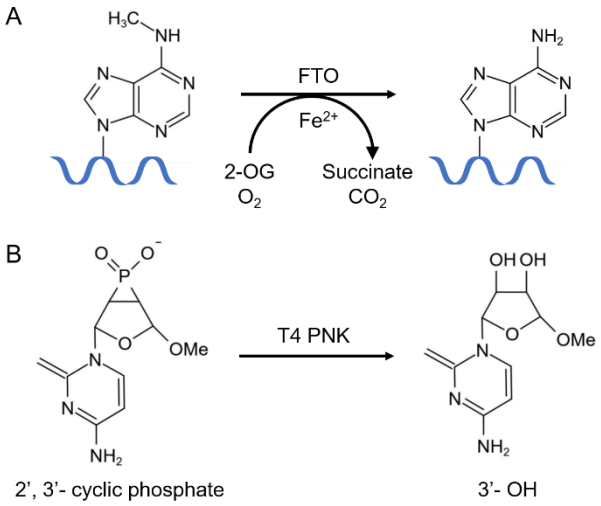

Fig. S1 (A) Pathways of the demethylation of the N6 of adenine in RNA probes catalyzed by FTO. (B) Pathways of the removal of 2',3' cyclic phosphate group from 3' the terminal of RNA by T4 PNK.

Optimization of experimental conditions

Optimization of experimental condition of FTO reaction. We investigated the effect of FTO reaction time upon the assay performance. The $F-F_0$ value is used to assess the assay performance, where F is the fluorescence intensity in the presence of 300 nM FTO and F_0 is the fluorescence intensity in the absence of FTO. As shown in Fig. S2, the $F-F_0$ value improves with reaction time from 20 to 150 min, reaches a plateau beyond 90 min. Thus, the reaction time of 90 min is used in subsequent researches.

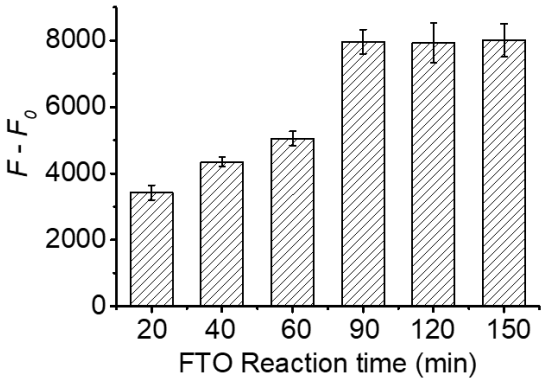

Fig. S2 Variance of the $F-F_0$ value with reaction time of FTO. Error bars represent the standard deviation of three experiments.

Optimization of experimental condition of cleavage reaction. As shown in Scheme 1, in the presence of FTO, MazF-mediated cleavage reaction produces large numbers of primers to trigger the PG-RCA reaction, and thus the experimental condition of MazF should be optimized. We investigated the effect of amount of MazF upon the assay performance. The $F-F_0$ value is used to assess the assay performance, where F is the fluorescence intensity in the presence of 300 nM FTO and F_0 is the fluorescence intensity in the absence of FTO. As shown in Fig. S3A, the $F-F_0$ value enhances with the increasing concentration of MazF from 4 to 12 U, and reaches a plateau beyond

the amount of 10 U. Thus, 10 U of MazF is used in subsequent researches. The reaction time of MazF was another key parameter for the proposed assay. As shown in Fig. S3B, the $F-F_0$ value enhances with the reaction time of MazF from 0.5 to 2.5 h, reaches a plateau beyond 1.5 h. Thus, 1.5 h is used as the reaction time of MazF in subsequent researches.

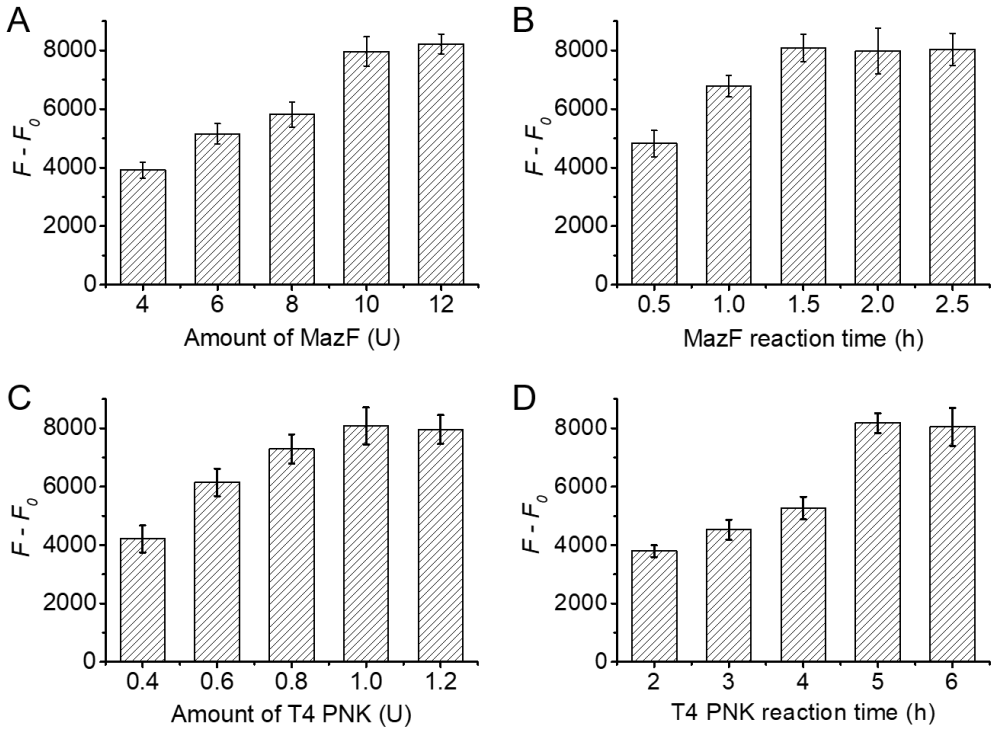

Fig. S3 (A) Variance of the $F - F_0$ value with different amounts of MazF. (B) Variance of the F − F_0 value with the reaction time of MazF. (C) Variance of the $F - F_0$ value with different amounts of T4 PNK. (D) Variance of the $F - F_0$ value with the reaction time of T4 PNK. Error bars represent the standard deviation of three experiments.

Optimization of experimental condition of dephosphorylation reaction. In order to obtain optimal amount of primers to initiate the PG-RCA reaction, we investigated the effect of amount of T4 PNK and the reaction time of T4 PNK upon the assay performance, respectively. The $F-F_0$ value is used to assess the assay performance, where F is the fluorescence intensity in the presence of 300

nM FTO and F_0 is the fluorescence intensity in the absence of FTO. As shown in Fig. S3C, the $F-F_0$ value enhances with the increasing concentration of T4 PNK from 0.4 to 1.2 U, and reaches a plateau beyond the amount of 1 U. Thus, 1 U of T4 PNK is used in subsequent researches. As shown in Fig. S3D, the $F-F_0$ value improves with the reaction time of T4 PNK from 1 to 6 h, reaches a plateau beyond 5 h. Thus, 5 h is the optimal reaction time of T4 PNK.

Optimization of experimental condition of PG-RCA reaction. To obtain the high amplification efficiency, a number of crucial conditions including the concentration of circular template, the amount of Vent (exo$^-$) DNA polymerase, the amount of Nb. BsmI, the concentration of dNTP, and the reaction temperature and reaction buffer of PG-RCA reaction were experimentally optimized. The $F-F_0$ value is used to assess the assay performance, where F is the fluorescence intensity in the presence of 300 nM FTO and F_0 is the fluorescence intensity in the absence of FTO. As shown in Fig. S4A, the $F-F_0$ value enhances with the increasing concentration of circular template and reaches the highest value at 60 nM, followed by the decrease beyond 60 nM. Thus, the optimal concentration of circular template is determined to be 60 nM. The close cooperation of DNA polymerase and nicking enzyme is crucial for efficient nucleic acid amplification. The concentration of vent (exo-) DNA polymerase influences the efficiency of PG-RCA reaction. As shown in Fig. S4B, the $F-F_0$ value improves with the increasing amount of Vent (exo-) DNA polymerase from 0.2 to 0.8 U, followed by the decrease beyond the amount of 0.8 U. Therefore, the optimal concentration of vent (exo-) DNA polymerase is determined to be 0.8 U. As shown in Fig. S4C, the $F-F_0$ value improves with the increasing amount of Nb. BsmI from 5 to 15 U, followed by the decrease beyond the amount of 15 U. Thus, the optimal amount of Nb. BsmI is determined to be 15 U. As shown in

Fig. S4D, the $F-F_0$ value enhances with the increasing concentration of dNTP from 400 to 800 μM, reaches a plateau beyond 600 μM. Thus, the optimal concentration of dNTP is determined to be 600 μM. Moreover, we investigated the effect of reaction temperature upon the $F-F_0$ value. As shown in Fig. S4E, the $F-F_0$ value enhances with the reaction temperature from 37 to 45 °C, followed by the decrease beyond 45 °C. The decrease of $F-F_0$ value may be attributed to the denaturation of duplex helixes at high temperature. Thus, 45 °C is used as the optimal reaction temperature in subsequent researches.

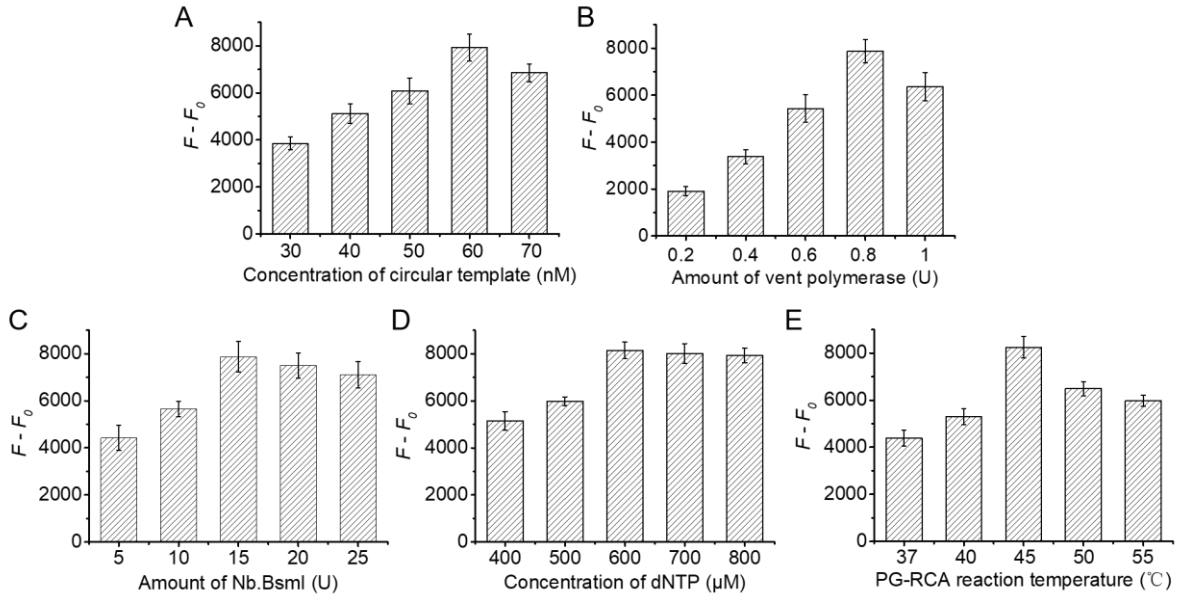

Fig. S4 (A) Variance of the $F - F_0$ value with different concentrations of circular template. (B) Variance of the $F - F_0$ value with different amounts of Vent (exo-) DNA polymerase. (C) Variance of the $F - F_0$ value with different amounts of Nb. BsmI. (D) Variance of the $F - F_0$ value with different concentrations of dNTP. (D) Variance of the $F - F_0$ value with different reaction temperature of PG-RCA. Error bars represent the standard deviation of three experiments.

Table S2. Comparison of the proposed method with the reported RNA demethylases assays.

Detection method	Target	Linear range	Detection limitation	Reference
fluorescent methylation-switchable probe-based assay	FTO	1 – 25 nM	10 nM	1
hybridization chain reaction-based fluorescence method	FTO	20 – 200 nM	2.273 nM	2
epigenetically responsive DNAzyme system-based fluorescence image assay	FTO	0 – 20 nM	0.5 nM	3
single-quantum-dot -based FRET sensor	FTO	1×10^{-13} – 1×10^{-6} M	7.9×10^{-14} M	4
MazF/nano-graphene oxide hybrid system-based fluorescence assay	ALKBH5	0 – 2 μM	/	5
Label-free fluorescence assay	FTO	1×10^{-5} – 1 nM	7.62×10^{-6} nM	This work

Detection selectivity.

We used uracil-DNA glycosylase (UDG), alkaline phosphatase (ALP), Dam DNA methyltransferases (Dam MTase), bovine serum albumin (BSA) and immunoglobulin G (IgG) as the interferences to investigate the selectivity of the proposed method. BSA and IgG are two nonspecific proteins. ALP can catalyze the dephosphorylation of various phosphorylated substrates (e.g., proteins, carbohydrates, and nucleic acids).[6] UDG can specifically recognize and excise uracil by catalyzing the cleavage of glycosidic bond between uracil and DNA backbone.[7] Dam MTase can catalyze the transfer of methyl group to adenine residues in specific genomic DNA sequences with S-adenosyl-L-methionine as the methyl donor.[8] As shown in Fig. 3A, no distinct fluorescence signal

is detected in the presence of BSA (Fig. 3A, red column), IgG (Fig. 3A, green column), UDG (Fig. 3A, blue column), ALP (Fig. 3A, magenta column), and Dam (Fig. 3A, cyan column) , while the presence of FTO generates a high fluorescence signal (Fig. 3A, yellow column), suggesting the good selectivity of the proposed method towards FTO.

Kinetic analysis. We employed the proposed method to evaluate the enzyme kinetic parameters of FTO. When ~80% of the substrate is unconsumed, the reaction is in the initial rate regime. We measured the initial velocity (V) in the presence of 100 nM FTO and different concentrations of the RNA probe in the range from 300 to 2000 nM for 10 min at 30 ℃. As shown in Fig. 3B, the enzyme kinetic parameters of FTO are obtained by fitting the data to the Michaelis–Menten equation $V = V_{max}[S]/(K_m + [S])$, where V_{max} is the maximum initial velocity, [S] is the substrate concentration, and K_m is the Michaelis–Menten constant. The V_{max} value is calculated to be 19.97 nM/ min and the K_m value is calculated to be 670.37 nM for FTO. The K_{cat} value is calculated to be 0.20 min^{-1} based on the equation $K_{cat} = V_{max}/[enzyme]$, where [$enzyme$] is the concentration of FTO. The measured K_m and K_{cat} values are consistent with those obtained by HPLC (K_m = 0.409 ± 0.023 μM; K_{cat} = 0.296 ± 0.004 min^{-1}),[9] suggesting that this method can be used to accurately evaluate the kinetic parameters of FTO.

References

1. A. Cheong, J. J. A. Low, A. Lim, P. M. Yen and E. C. Y. Woon, *Chem. Sci.*, 2018, **9**, 7174-7185.

2. L. Zhao, T. Fan, Y. Han, Y. Wang, Y. Jiang and F. Liu, *Sens. Actuator B-Chem.*, 2021, **341**, 129983.

3. Q. Wang, K. Tan, H. Wang, J. Shang, Y. Wan, X. Liu, X. Weng and F. Wang, *J. Am. Chem. Soc.*, 2021, **143**, 6895-6904.

4. Y. Zhang, Q.-n. Li, K. Zhou, Q. Xu and C.-y. Zhang, *Anal. Chem.*, 2020, **92**, 13936-13944.

5. S.-H. Yim, H. J. Cha, S.-J. Park, Y. Yim, J.-S. Woo and D.-H. Min, *Chem. Commun.*, 2020, **56**, 4716-4719.

6. F. Ma, W.-j. Liu, L. Liang, B. Tang and C.-Y. Zhang, *Chem. Commun.*, 2018, **54**, 2413-2416.

7. L.-j. Wang, M. Ren, Q. Zhang, B. Tang and C.-y. Zhang, *Anal. Chem.*, 2017, **89**, 4488-4494.

8. L.-j. Wang, X. Han, C.-c. Li and C.-y. Zhang, *Chem. Sci.*, 2018, **9**, 6053-6061.

9. G. Jia, Y. Fu, X. Zhao, Q. Dai, G. Zheng, Y. Yang, C. Yi, T. Lindahl, T. Pan, Y. G. Yang and C. He, *Nat. Chem. Biol.*, 2011, **7**, 885-887.